# Selective Catalytic Reduction of NO with Propene over $Au/CeO_2/Al_2O_3$ Catalysts

**Xinkui Wang[1,2], Aiqin Wang[1], Xiaodong Wang[1], Xuefeng Yang[2] and Tao Zhang[1]***

[1] State Key Laboratory of Catalysis, Dalian Institute of Chemical Physics, Chinese Academy of Sciences, Dalian 116023, China. E-mail: taozhang@dicp.ac.on

[2] Laboratory of Plasma Physical Chemistry, Dalian University of Technology, Dalian 116023, China

## Abstract

**Selective catalytic reduction of NO by propene under an oxygen-rich atmosphere has been investigated over $Au/CeO_2$, $Au/CeO_2/Al_2O_3$ and $Au/Al_2O_3$ catalysts prepared by deposition-precipitation. The results demonstrated that $Au/16\%CeO_2/Al_2O_3$ had good low-temperature activity, selectivity towards $N_2$ and stability, which is superior to that of $Pt/Al_2O_3$. It was also found that adding 2% water vapour to the feed stream enhanced the NO conversions at low temperatures while the presence of 20 ppm $SO_2$ increased NO conversions at higher temperatures. It is particularly interesting that under the simultaneous presence of 2% water vapour and 20 ppm $SO_2$, the NO conversions to $N_2$ were significantly increased and the temperature window was widened significantly. The catalysts were characterized by X-ray diffraction (XRD), high resolution transmission electron microscopy coupled with energy dispersive X-ray spectroscopy (HRTEM-EDX) and temperature-programmed reduction ($H_2$-TPR) techniques. Both XRD and HRTEM revealed that $CeO_2$ was highly dispersed on the alumina support, and HRTEM combined with EDX showed that gold particles were preferentially deposited on those highly dispersed $CeO_2$ particles. The gold deposition made $CeO_2$ more reducible and interaction between gold and those highly dispersed $CeO_2$ particles became stronger than that with the bulk $CeO_2$, and this interaction is probably responsible for the superior catalytic performance of the $Au/CeO_2/Al_2O_3$.**

## Keywords

Gold, Ceria, SCR, NO, Propene

## Introduction

Selective catalytic reduction of NO by hydrocarbons in the presence of excess oxygen (HC-SCR) is considered as a potentially promising way to remove $NO_x$ from automobile exhaust. Among the various catalysts investigated, supported platinum–based catalysts have shown the highest activities at low temperatures (between 200°C and 350°C) in the tests on a diesel engine working in an urban cycle (1). However, the high selectivity to $N_2O$ over the Pt-based catalysts largely limited their applications, since $N_2O$ contributes significantly to a greenhouse effect. Consequently, much work has been done to increase the selectivity to $N_2$ and limit the production of $N_2O$ at low temperatures by varying the nature of the support, the preparation method or by using various hydrocarbons as the reductants (2-5).

In the last decade, catalysis by gold has been the hotspot in the heterogeneous catalysis field due to its exceptionally high activities at low temperatures, in particular for CO oxidation (6). We believe that such a unique feature of gold catalysts has a close relationship with the weak adsorption of most reactant molecules on gold nanoparticles. Another advantage that the use of gold catalysts offer compared to Pt catalysts is the lower cost and greater price stability of gold, which is important in their application for automobile emission control. However, in contrast with the extensively studied low-temperature CO oxidation, NO reduction with hydrocarbons under an oxygen-rich atmosphere has been less studied over nanogold catalysts although oxide supported gold nanoparticles have been found to give good catalytic performances at both high and relatively low temperature (7,8). Among the various catalysts investigated, Au/ZnO prepared by co-precipitation has shown the best low temperature catalytic activity, which gives a maximum NO conversion of 25% at 250°C (7). However, over Au/ZnO, $N_2O$ is also formed and ZnO support is less thermally stable compared with alumina when exposed to high-temperature emissions. Therefore, ZnO is not the best choice as a catalyst support for automotive emission control. On the other hand, it is well known that ceria-alumina is one of the best supports of three way catalysts used for the elimination of pollutants in automobile exhausts onto which precious metals (typically Rh, Pt and/or Pd) are dispersed (9). Ceria is a structural promoting component. It enhances the metal dispersion and participates in the stabilization of the alumina support against thermal sintering (10,11). On the other hand, the addition of ceria to alumina induces a modification of the electronic density of the aluminium cations, implying a change in the acid-base properties of the support surface (12). In addition, the well established catalytic and redox properties of the $Ce^{3+}/Ce^{4+}$ couple, makes $CeO_2/Al_2O_3$ a suitable support for obtaining

well dispersed and active gold catalyst for the oxidation of CO and volatile organic compounds (13,14).

In the present work, which has the objective of combining the above advantages of gold nanocatalysts with those of the $CeO_2/Al_2O_3$ support, we attempt to prepare highly dispersed gold nanoparticles on $CeO_2/Al_2O_3$ support and apply it to the HC-SCR reaction. We firstly prepared four gold-containing catalysts, $Au/CeO_2$, $Au/Al_2O_3$, $Au/5\%CeO_2/Al_2O_3$ and $Au/16\%CeO_2/Al_2O_3$ by deposition-precipitation. The catalytic activity tests showed that $Au/16\%CeO_2/Al_2O_3$ exhibited a good low-temperature activity and a high selectivity to $N_2$ for NO reduction with propene under an oxygen-rich atmosphere. Various characterization techniques including XRD, TEM, EDX, and $H_2$-TPR were employed to characterize the $Au/CeO_2/Al_2O_3$ catalysts.

## Experimental

### Preparation of the samples

The starting $\gamma$-$Al_2O_3$ powder was made in our laboratory and had a BET surface area of $228m^2/g$. $CeO_2$ powder was obtained by thermal decomposition of cerous nitrate at 650°C in the air for 4h, giving a BET surface area of $58m^2/g$. The composite support $CeO_2/Al_2O_3$ with various $CeO_2$ loadings was prepared by impregnation of the $\gamma$-$Al_2O_3$ with an aqueous solution of cerous nitrate. Following impregnation, the sample was dried at 120°C for 6h and then calcined in air at 500°C for 4h. Gold-containing catalysts were prepared by deposition-precipitation. An appropriate volume of an aqueous solution of $HAuCl_4$ ($1.6x10^{-3}$M) was adjusted to pH = 7 by dropwise addition of 1N NaOH solution. The resulting solution was heated to 70°C,and then 2g of the support powder ($Al_2O_3$,$CeO_2$ or $CeO_2/Al_2O_3$ ) was added. The resulting mixture was continuously stirred at 70°C for 16h. After filtration and repeated washing until no $Cl^-$ could be detected, the solid sample was dried at 120 °C for 12h and calcined at 500°C in $20\%O_2$/He for 1h.

### Characterization techniques

BET specific surface areas were measured by nitrogen adsorption at -196°C on a Micromeritics ASAP 2010 apparatus. Before analysis, the samples were degassed at 350°C for 4h.

Gold contents of the catalyst samples were determined by inductively coupled plasma spectrometer (ICP-AES).

XRD patterns were obtained on a Rigaku D/MAX-2500/PC powder X-ray diffractometer using a Cu $K_\alpha$ radiation source ($\lambda$ = 0.15432 nm), operated at 40kV and 250mA. The samples were scanned in the $2\theta$ range from 10 to 80°C.

Gold particle size was examined using HRTEM (FEI TECNAI $G^2$ F30, operated at 320 kV). The samples were ultrasonically dispersed in ethanol and dropped on a copper grid coated with a carbon film.

$H_2$-TPR experiments were carried out on a Micromeritics Auto ChemΠ2920. 0.15g of the sample was pretreated at 200°C in an Ar stream for 1h in order to remove surface contaminants. After cooling to room temperature under Ar, the gas flow was switched to $10\%H_2$/Ar at a flow rate of 30ml/min, and the temperature was raised at a rate of 10°C/min up to 1000°C. The consumption of $H_2$ was recorded with TCD.

### Catalytic measurements

Catalytic activity measurements were carried out using a fixed-bed flow reactor. A reactant gas mixture containing 1000ppm NO, 1000ppm $C_3H_6$, $5\%O_2$, 0 or $2\%H_2O$ and 0 or 20ppm $SO_2$ in helium passed through 0.15g catalyst at a flow rate of 100mL/min, corresponding to a space velocity of $30,000h^{-1}$. The effluent gas mixture was analysed using an on-line gas chromatograph (HP6890) equipped with TCD and FID.

## Results and Discussion

### Effect of $CeO_2$ addition on the gold loading

Table 1 indicates the gold loadings (determined by ICP-AES) and BET surface areas of the catalyst samples. We noticed that the actual gold contents in the four catalyst samples are all far lower than the desired value (2.4 wt%), indicating that a low loading efficiency resulted from the deposition-precipitation process. Moreover, with the addition of $CeO_2$ to the $Al_2O_3$ support, the gold loading increased from 0.6 wt% to 1.0%, and it was 1.4% on the pure $CeO_2$ support. This can be explained by the more basic character of $CeO_2$ compared to alumina. In fact, it has been described that when cerium is in direct contact with alumina, cerium-oxygen bonds are more basic than aluminate-type ligands since Ce is less electronegative than Al (15,16). In this respect, the basicity of ceria may contribute to the difference in the gold loading. On the other hand, the higher gold loading on the ceria support also implies a stronger interaction between gold particles and the ceria support, probably due to the oxygen vacancy of the ceria support (17). Clearly, addition of ceria to the alumina support can significantly modify its surface nature, inducing more gold particles to be deposited on it.

### Gold particle size distribution on the $Au/CeO_2/Al_2O_3$

Figure1 depicts the wide-angle XRD patterns of the samples. For the $Au/CeO_2$, a very weak and broad peak at 38.2° due to crystalline gold can be observed in addition to the diffraction lines of $CeO_2$ (Figure1A), indicating a very small

**Table 1**

*Gold loading and BET surface area of the samples.*

| Sample | Au wt% | $S_{BET}(m^2/g)$ |
|---|---|---|
| $Au/CeO_2$ | 1.4 | 58 |
| $Au/Al_2O_3$ | 0.6 | 227 |
| $Au/5\%CeO_2/Al_2O_3$ | 0.9 | 226 |
| $Au/16\%CeO_2/Al_2O_3$ | 1.0 | 190 |

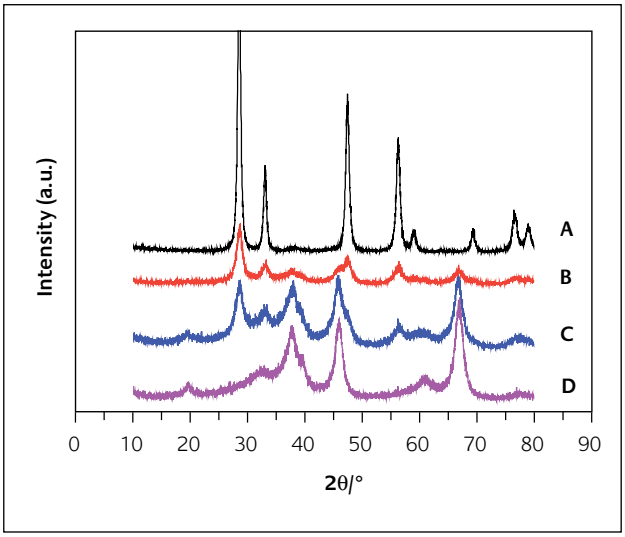


**Figure 1**

*XRD patterns of 1.4% Au/$CeO_2$ (A), 1.0%Au/16%$CeO_2$ /$Al_2O_3$ (B), 0.9% Au/5%$CeO_2$/$Al_2O_3$ (C) and 0.6%Au/$Al_2O_3$ (D).*

gold particle size. For the other three samples with $Al_2O_3$ as the main component of the support (Figures 1B, C and D), we cannot observe gold diffraction lines because the strongest diffraction line of gold at 38.2° (111) coincidentally overlaps with the γ-$Al_2O_3$ diffraction line. On the other hand, compared with XRD peaks of Au/$CeO_2$, both the Au/5%$CeO_2$/$Al_2O_3$ and the Au/16%$CeO_2$/$Al_2O_3$ exhibited broadened $CeO_2$ peaks. From Scherrer's equation, ceria particle size was estimated to be about 13 nm in the Au/$CeO_2$ sample, while it was only about 7 nm on the Au/16%$CeO_2$/$Al_2O_3$ (Figure1B). Thus, $CeO_2$ was highly dispersed on the $Al_2O_3$ support.

Figure 2 shows the HRTEM images of the Au/$Al_2O_3$ and the Au/16%$CeO_2$/$Al_2O_3$. From Figure 2A we can see that gold particles with a size of 3-5nm are highly dispersed onto the alumina support. This is in agreement with the literature (18). However, for the Au/16%$CeO_2$/$Al_2O_3$ sample, it is difficult to distinguish gold particles from the ceria particles because of the high atomic weight of the cerium atom. From the HRTEM image (Figure 2B) of 1.0%Au/16%$CeO_2$/$Al_2O_3$, the ceria particles with a lattice fringe of 0.32 nm can be clearly observed (19), and the particle size of ceria is 6-8 nm, consistent with the XRD results. In addition, gold particles with a lattice fringe of 0.23 nm and a particle size of 3-5nm can be identified (19). To confirm the presence of gold particles on the ceria support, we performed the STEM (bright field) on the 1.0%Au/16%$CeO_2$/$Al_2O_3$ sample, as shown in Figure 3. The bright particles in the image correspond to the ceria or gold, while the dark parts are due to the alumina support. The EDX analysis on the selected bright spot shows that the bright spot is mainly composed of gold and ceria. In fact, examination on various parts of the image with EDX revealed that gold is always present associated with the ceria. This result implies that gold particles are preferentially deposited onto the ceria phase in the $CeO_2$/$Al_2O_3$ composite, again demonstrating the stronger interaction between gold and the ceria. The higher gold loading on the ceria-containing support also supports this conclusion. A similar conclusion was arrived at by Centeno et al (13,14) from EDX and XPS results.

### $H_2$-TPR results

$H_2$-TPR profiles of the Au/$CeO_2$, Au/$Al_2O_3$, Au/5%$CeO_2$/$Al_2O_3$ and Au/16%$CeO_2$/$Al_2O_3$ are illustrated in Figure 4, and those of the corresponding supports are shown in Figure 5. The TPR profile of pure $CeO_2$ (Figure 5A) contains two peaks: a low temperature (LT) peak at $T_{max}$= 488°C assigned to the reduction of surface $CeO_2$ and a high temperature (HT) peak at $T_{max}$=840°C due to the reduction of bulk ceria (20). When ceria was deposited onto the alumina support, the

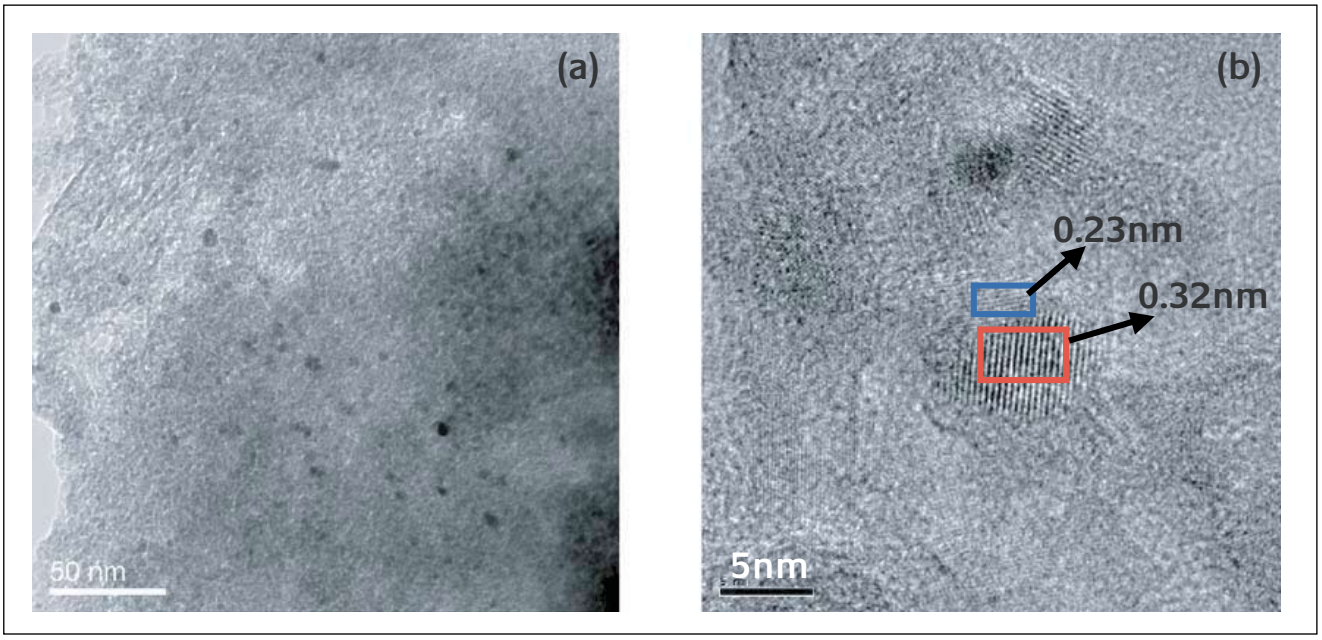


**Figure 2**

*HRTEM photographs of 0.6% Au/$Al_2O_3$ (A) and 1.0%Au/16%$CeO_2$ /$Al_2O_3$ (B)/.*

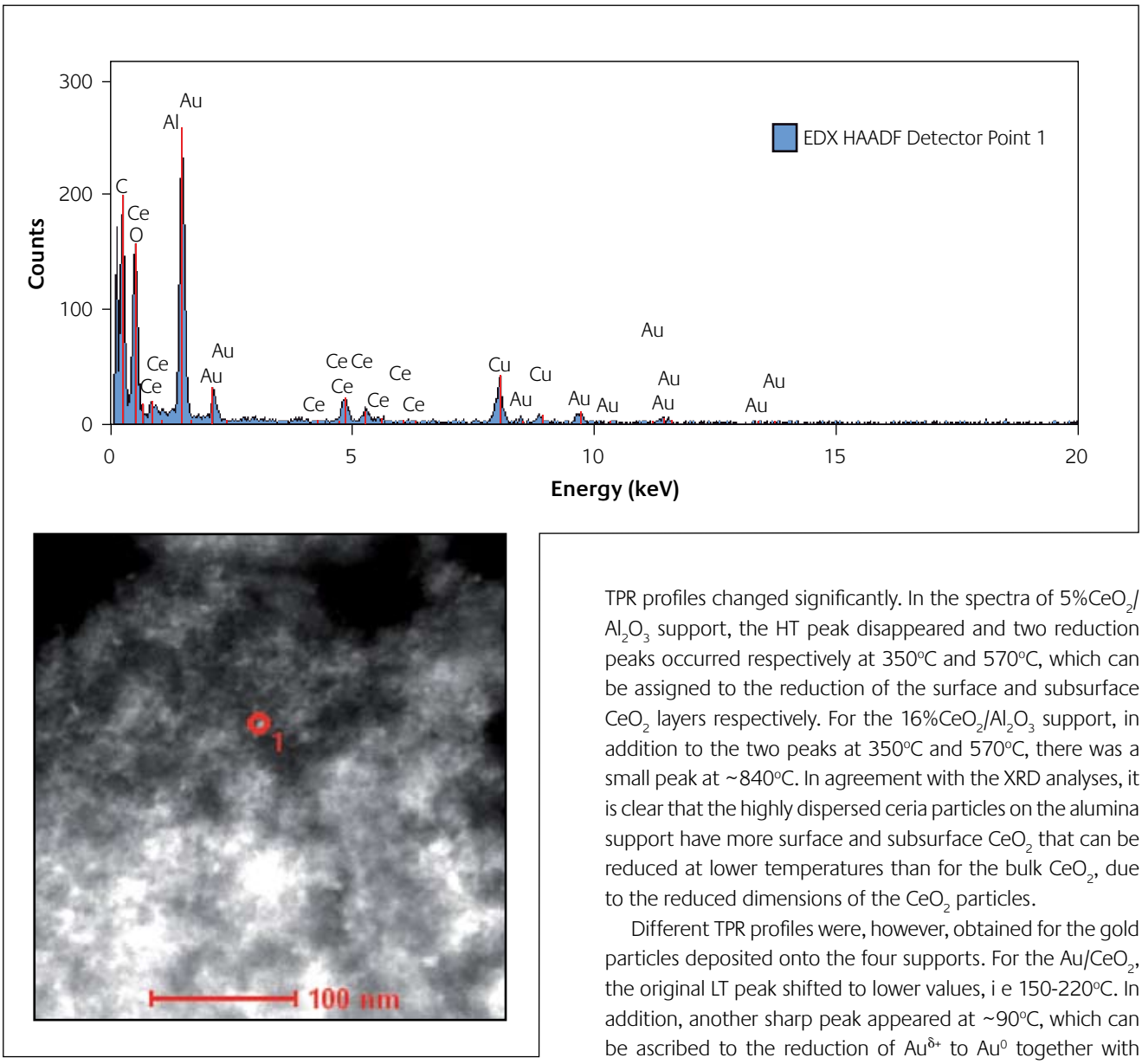


**Figure 3**
*Typical STEM image and EDX analysis of 1.0%Au/16%$CeO_2$/$Al_2O_3$.*

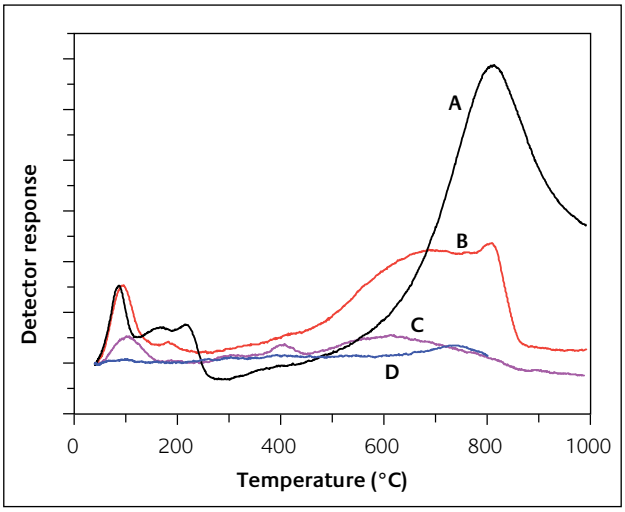


**Figure 4**
*$H_2$-TPR profiles of 1.4% Au/$CeO_2$(A), 1.0% Au/16%$CeO_2$/$Al_2O_3$(B) 0.9% Au/5%$CeO_2$/$Al_2O_3$(C) and 0.6% Au/$Al_2O_3$(D).*

TPR profiles changed significantly. In the spectra of 5%$CeO_2$/$Al_2O_3$ support, the HT peak disappeared and two reduction peaks occurred respectively at 350°C and 570°C, which can be assigned to the reduction of the surface and subsurface $CeO_2$ layers respectively. For the 16%$CeO_2$/$Al_2O_3$ support, in addition to the two peaks at 350°C and 570°C, there was a small peak at ~840°C. In agreement with the XRD analyses, it is clear that the highly dispersed ceria particles on the alumina support have more surface and subsurface $CeO_2$ that can be reduced at lower temperatures than for the bulk $CeO_2$, due to the reduced dimensions of the $CeO_2$ particles.

Different TPR profiles were, however, obtained for the gold particles deposited onto the four supports. For the Au/$CeO_2$, the original LT peak shifted to lower values, i e 150-220°C. In addition, another sharp peak appeared at ~90°C, which can be ascribed to the reduction of $Au^{\delta+}$ to $Au^0$ together with the reduction of surface ceria (21-23). For the other two Au/$CeO_2$/$Al_2O_3$ catalysts, the reduction peaks of $Au^{\delta+}$ to $Au^0$ as well as the reduction of surface ceria are also observed at ~100°C. Different from the Au/$CeO_2$/$Al_2O_3$ catalysts, when Au was deposited onto the pure $Al_2O_3$ support, no reduction peaks can be observed on the Au/$Al_2O_3$ within the whole investigated temperature range (Figure 4D), indicating the metallic state of Au. The presence of $Au^{\delta+}$ on the $CeO_2$-containing support reflects the strong interaction between gold and ceria. It has been reported that the high activity of Au/$CeO_2$/$Al_2O_3$ catalysts might be related to the capacity of Au nanoparticles to weaken the Ce-O bond. Thus, the mobility/reactivity of the surface lattice oxygen is increased by the presence of gold, and this even makes the gold particles, probably on the oxygen vacancies, oxidized to some extent (21,24) .

## Catalytic activity

In this work, we firstly compared the catalytic performances of gold particles on different supports: $Al_2O_3$, $CeO_2$, 5%$CeO_2$/$Al_2O_3$ and 16%$CeO_2$/$Al_2O_3$, for NO reduction with propene in

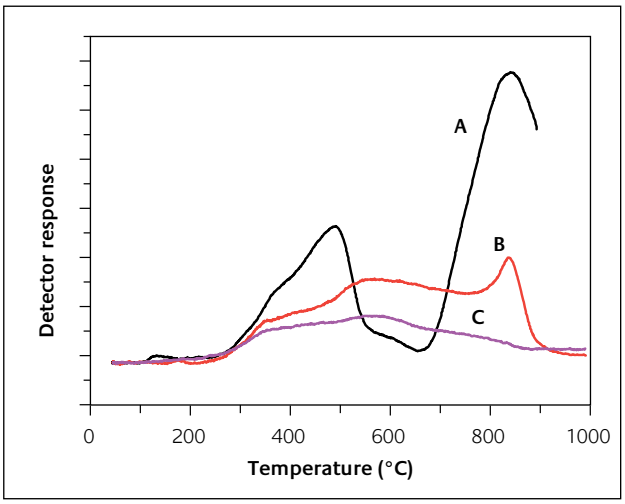


**Figure 5**

*$H_2$-TPR profiles of $CeO_2$ (A), 16%$CeO_2$/$Al_2O_3$ (B) and 5%$CeO_2$/$Al_2O_3$ (C).*

the presence of excess oxygen. Figure 6 (A, B, C) illustrates the conversions of NO to $N_2$ and $N_2O$ and the conversions of $C_3H_6$ as a function of the reaction temperature. It is clear that Au/$CeO_2$ has a very low selectivity to $N_2$ but a comparatively high selectivity to $N_2O$. For example, the maximum NO conversion to $N_2$ was only 5% at 200°C, while the conversion to $N_2O$ reached 26% at 250 °C. In contrast, the catalytic performance of Au/$Al_2O_3$ is very different from that of Au/$CeO_2$. NO conversion to $N_2$ was at the highest value of 47% at 450 °C on the Au/$Al_2O_3$, while only a small amount of $N_2O$ (< 5%) was produced at low temperatures (< 200 °C). Different from either Au/$CeO_2$ or Au/$Al_2O_3$, when $CeO_2$/$Al_2O_3$ was used as the support, the catalytic activities of gold at low temperatures were enhanced greatly. For example, the maximum NO conversion to $N_2$ over the 1.0%Au/16%$CeO_2$/$Al_2O_3$ was 46% at 250 °C, and $N_2O$ formation was negligible in the whole temperature range. Obviously, the high selectivity to $N_2$ obtained on the Au/$CeO_2$/$Al_2O_3$ seems to be associated with the presence of the composite support $CeO_2$/$Al_2O_3$. It has been suggested that ceria is able to promote NO reduction to $N_2O$ via the following route (25):

$$2[Ce^{3+}\text{-}(v)]+2NO \rightarrow Ce^{4+}\text{-}[ONNO]^{2-}\text{-}Ce^{4+}$$
$$Ce^{4+}\text{-}[ONNO]^{2-}\text{-}Ce^{4+} \rightarrow (Ce^{4+}\text{-}O^{2-}) + [Ce^{4+}\text{-}(v)] + N_2O$$

Consequently, a significant proportion of the $N_2O$ formed on the Au/$CeO_2$ sample may be related to the oxygen vacancies in the $CeO_2$ support: but with Au/$Al_2O_3$, the formation of $N_2O$ may follow a different path where a dissociative adsorption of NO on gold particles is involved (26,27). When a $CeO_2$/$Al_2O_3$ composite was employed as the support, the decreased oxygen vacancies can only partly explain the negligible production of $N_2O$ (9). Other reasons may lie in the synergistic effect between $Al_2O_3$ and $CeO_2$ and these interpretations need to be further explored.

On the other hand, we can see from Figure 6C that $C_3H_6$ conversions were largely promoted by the presence of $CeO_2$. For example, a complete conversion of $C_3H_6$ was obtained

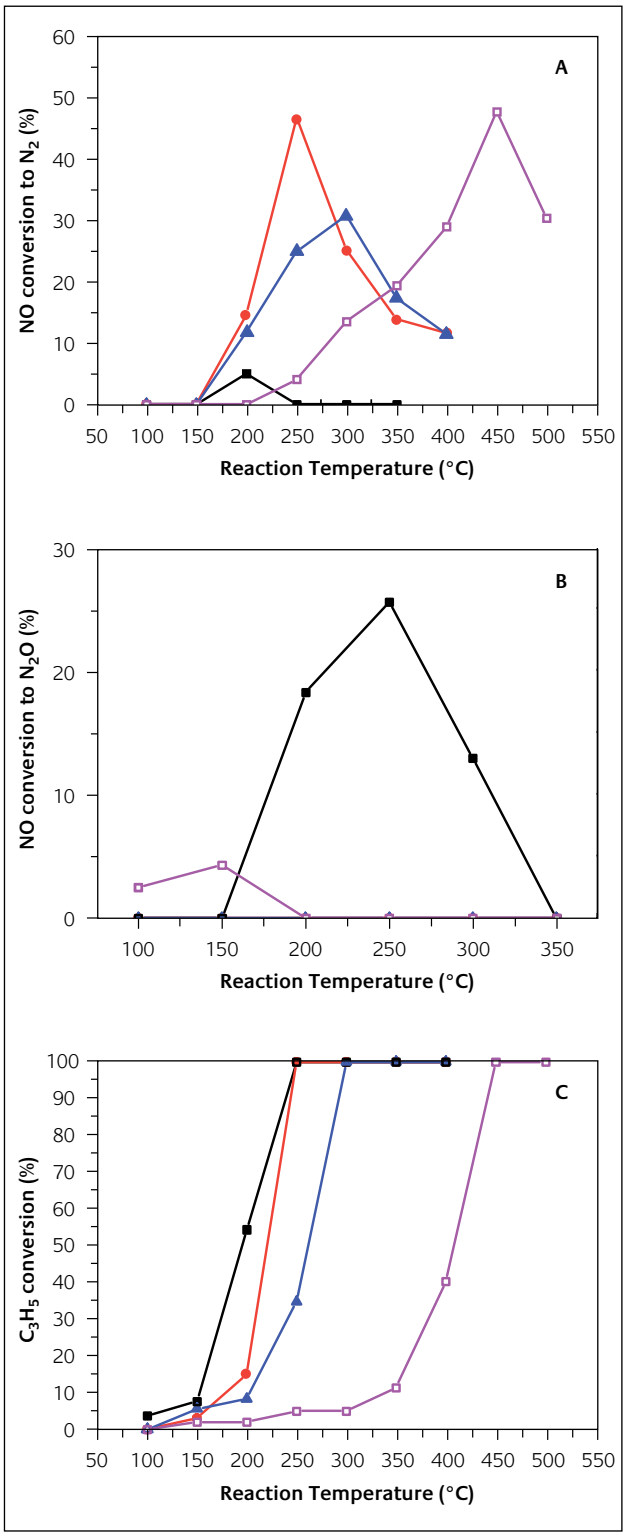


**Figure 6**

*Reaction temperature dependence of NO conversion to $N_2$ (A) and $N_2O$ (B) and $C_3H_6$ conversion to $CO_2$ (C) over 0.15g 1.4%Au/$CeO_2$ (■), 1.0%Au/16%$CeO_2$/$Al_2O_3$ (●), 0.9%Au/5%$CeO_2$/$Al_2O_3$ (▲) and 0.6%Au/$Al_2O_3$ (□.) Feed conditions: 1000ppm NO, 1000ppm $C_3H_6$, 5% $O_2$ and He balance (vol%), total flow rate = 100ml $min^{-1}$.*

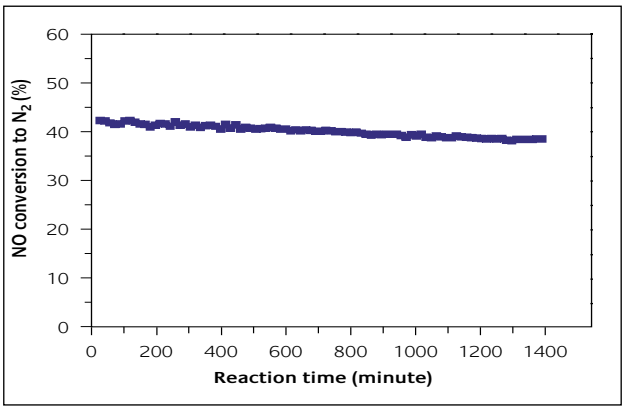


**Figure 7**

*NO conversion to $N_2$ over 1.0%Au/16%$CeO_2$/$Al_2O_3$ catalyst as a function of reaction time at 250 °C.*

at 250 °C over the Au/16%$CeO_2$/$Al_2O_3$, while it was realized at 450 °C over the Au/$Al_2O_3$. Comparing Figure 6A with Figure 6C, it can be seen that the maximum NO conversions are always associated with the complete conversion of $C_3H_6$. In agreement with our observations, Gluhoi et al. also found that Au/$CeO_2$/$Al_2O_3$ catalyst performed very well for the propene oxidation reaction (28). Such a high activity of the Au/16%$CeO_2$/$Al_2O_3$ in the complete oxidation of propene led to a low selectivity of $C_3H_6$ towards NO reduction. In fact, the selectivity of $C_3H_6$ towards NO reduction at 250 °C was only 23%.

Additionally, with a difference in the ceria content, the catalytic activity differs slightly. The sample with larger proportion of ceria (1.0%Au/16%$CeO_2$/$Al_2O_3$) shows higher catalytic activity, which may be related with the fact that Au/$CeO_2$ is more active than the Au/$Al_2O_3$ for propene oxidation (Figure 6C).

The stability of Au/16%$CeO_2$/$Al_2O_3$ was also investigated. From Figure 7, we can see that after a 1350min-run, the NO conversion only slightly dropped from 42% to 39%, indicating good stability. The presence of ceria prevents the agglomeration of gold, which is the main reason for the improved stability.

It is known that both $SO_2$ and water vapour are present in automotive emissions. It was, therefore, important to investigate the effect of these two components in the feed stream on the catalytic performance of our Au/$CeO_2$/$Al_2O_3$ sample. Figure 8 illustrates the conversions of NO and $C_3H_6$ with reaction temperature over the Au/16%$CeO_2$/$Al_2O_3$ in the presence of 2% water vapour or 20 ppm $SO_2$, and also in the simultaneous presence of the two components. Compared with the dry feed gas, it is interesting that the NO conversions in the low temperature range (100-200°C) were enhanced by the presence of moisture in the feed gas, whereas they were decreased at 250°C. The positive effect of $H_2O$ on the NO conversion over the Au/$CeO_2$/$Al_2O_3$ at low temperatures is very similar to the case of CO oxidation over Au/$Al_2O_3$, which may be related to the creation of active Au species promoted by $H_2O$ (18,29). Different from the influence of moisture, the presence of 20 ppm $SO_2$ greatly widened the temperature

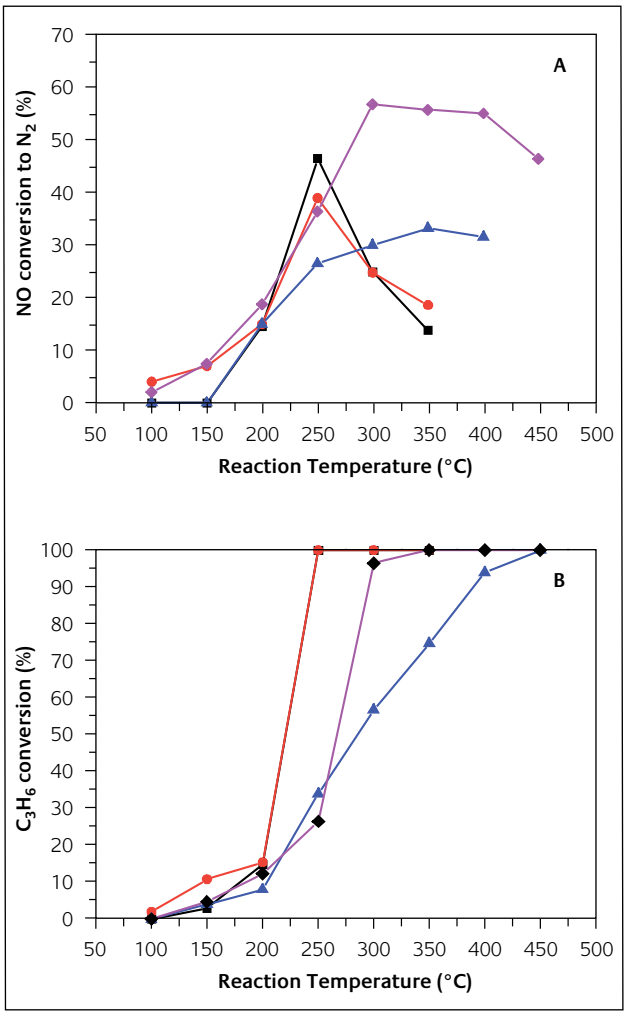


**Figure 8**

*Reaction temperature dependence of NO conversions to $N_2$ (A) and $C_3H_6$ conversions (B) over 0.15g 1.0%Au16% /$CeO_2$ /$Al_2O_3$ catalyst under the absence (■) or presence of 2%$H_2O$ (●) or 20ppm$SO_2$ (▲) or simultaneous presence of 2%H2O and 20ppm$SO_2$ (◆) in the feed stream. Gas composition: 1000ppm NO+ 1000ppm $C_3H_6$ +5%$O_2$, He as a balance.*

window in spite of the fact that the maximum NO conversion decreased from 46% to 33%. To our surprise, under the simultaneous presence of 2% water vapor and 20 ppm $SO_2$, the NO conversions to $N_2$ were significantly increased, with the maximum NO conversion of 56% at 300 °C. Meanwhile, the temperature window was largely widened (250~450 °C). From Figure 8B, we can see that the $C_3H_6$ conversions were largely decreased by the addition of $SO_2$, suggesting that the presence of $SO_2$ suppress the combustion of $C_3H_6$ by $O_2$ and increases the selectivity of $C_3H_6$ towards NO reduction. It has been reported that the tolerance of metal oxide-based catalysts to $SO_2$ presence in the feed depends on the type and oxidation state of the deposited metal, and the nature of the support (30,31). In the case of Au/$CeO_2$/$Al_2O_3$, the enhanced activity and selectivity obtained by the addition of $SO_2$ may be caused by the selective or preferential poisoning of active sites for $C_3H_6$ combustion. This result provides some hints that NO reduction and $C_3H_6$ combustion occur at different sites.

In summary, the modification of alumina support with the ceria greatly improved the catalytic performance of gold particles in the NO reduction with propene. From the above XRD, TEM and TPR characterizations, we know that ceria was highly dispersed onto the alumina support, and this results in the easy reduction of not only surface ceria but also subsurface ceria. It has been suggested that the reduction of subsurface ceria is associated with the creation of oxygen vacancies, and gold preferentially deposited onto these sites helped by the strong interaction between the oxygen vacancies and gold particles. Therefore, the superior behaviour of $Au/CeO_2/Al_2O_3$ can be attributed to the improved interaction between gold and ceria particles. Such a catalytic performance is superior to that of Pt-group metal catalysts (1-5), on which a significant amount of $N_2O$ (about 30%) was formed under similar conditions. Such a high catalytic activity and selectivity to $N_2$, combined with the excellent resistance to poison by water vapour and sulfur dioxide, makes $Au/CeO_2/Al_2O_3$ catalysts promising candidates for an effective 'cold start' application.

## Conclusions

Highly dispersed ceria particles on alumina were prepared by impregnation, and then gold particles were deposited on this $CeO_2/Al_2O_3$ composite support. HRTEM-EDX measurements indicated that gold was preferentially deposited onto the ceria particles due to the improved interaction between gold and ceria nanoparticles. The $Au/CeO_2/Al_2O_3$ exhibited high activity and selectivity to $N_2$ at low temperatures, as well as good stability and resistance to poisoning by water and sulfur dioxide. These characteristics makes this catalyst a promising candidate for solving 'cold-start' problems in automobile emission control.

## Acknowledgements

Supports of National Science Foundation of China (NSFC) for Distinguished Young Scholars (No. 20325620) and NSFC grant (No.20673116) are gratefully acknowledged

## About the authors

**Professor Tao Zhang** is the Director of Dalian Institute of Chemical Physics, Chinese Academy of Sciences. His research interests are in heterogeneous catalysis, particularly in environmental catalysis.

## References

1 A. Obuchi, A. Ohi, M. Nakamura, A. Ogata, K. Mizuno and H. Ohuchi, *Appl. Catal. B*, 1993, **2**, 71
2 R. Burch and T.C. Watling, *Appl. Catal. B*, 1997, **11**, 207
3 P. Denton, A. Giroir-Fendler, H. Praliaud and M. Primet, *J. Catal*., 2000, **189**, 410
4 E. Seker and E. Gulari, *J. Catal*., 2000, **194**, 4
5 R. Burch and D. Ottery, *Appl. Catal. B*, 1997, **13**, 105
6 M. Haruta, N. Yamada, T. Kobayashi and S. Iijima, *J. Catal*., 1998, **115**, 301
7 A. Ueda, T. Oshima and M. Haruta, *Appl. Catal. B*, 1997, **12**, 81
8 A. Ueda and M. Haruta, *Gold Bull*.,1999, **32**, 3
9 A. Trovarelli, *Catal. Rev.- Sci. Eng*., 1996, **38,** 439
10 R. Dictor and S. Roberts, *J. Phys. Chem*. 1989, **93**, 5846
11 A. Martinez-Arias, M. Fernández-García, L.N. Salamanca, R.X. Valenzuela, J.C. Conesa and J. Soria, *J. Phys. Chem. B*, 2000, **104**, 4038
12 M.A. Centeno, P. Malet, I. Carrizosa and J.A. Odriozola, *J. Phys. Chem. B*, 2000, **104**, 3310
13 M.A. Centeno, C.Portales, I. Carrizosa and J.A. Odriozola, *Catal. Lett*., 2005, **102**, 289
14 M.A. Centeno, M.Paulis, M. Montes and J.A. Odriozola, *Appl. Catal.A*, 2002, **234**, 65
15 J. Soria, J.M. Coronado and J.C. Conesa, *J. Chem. Soc. Faraday Trans*., 1996, **92**, 1619
16 C.Morterra, V.Bolis and G.Magnacca, *J. Chem. Soc. Faraday Trans*., 1996, **92**, 1991
17 Z. Yan, S. Chinta, A.A. Mohamed, J. P. Fackler, Jr. and D.W. Goodman, *J .Am. Chem. Soc*., 2005, **127**, 1604
18 C.K. Costello, M.C. Kung, H.-S. Oh, Y. Wang and H.H. Kung, *Appl. Catal. A,* 2002, **232**, 159
19 S.-Y. Lai, Y. Qiu and S. Wang, *J. Catal*., 2006, **237**, 303
20 H.C. Yao and Y.F. Yao, *J .Catal*.,1984, **86**, 254
21 J. Guzman, S. Carrettin and A. Corma, *J. Am. Chem. Soc*., 2005, **127**, 3286
22 P. Concepción, S. Carrettin and A. Corma, *Appl. Catal. A*, 2006, **307**, 42
23 C. Milone, M. Fazio, A. Pistone and S. Galvagno, *Appl. Catal. B*, 2006, **68**, 28
24 S. Scire, S. Minico, C. Crisafulli, C. Satriano and A. Pistone, *Appl. Catal. B*, 2003, **40**, 43
25 A. Martinez-Arias, J. Soria, J.C. Conesa, X.L. Seoan, A. Arcoya and R. Cataluna, *J. Chem Soc. Faraday Trans*., 1995, **91**, 1679
26 B.K. Cho, B.H. Shanks and J.E. Bailey, *J.Catal*., 1989, **115**, 486
27 R. Burch, P.J. Millington, and *A.P. Walker, Appl.Catal.B*, 1994, **4**, 65
28 A.C. Gluhoi, N. Bogdanchikova and B.E. Nieuwenhuys, *J.Catal*., 2005, **229**, 154
29 H.-S. Oh, C.K. Costello, C. Cheung, H.H. Kung and M.C. Kung, *Stud. Surf. Sci. Catal*. 2001, **139**, 375
30 E.A. Efthimiadis, G.D. Lionta, S.C. Christoforou and I.A. Vasalos, *Catal. Today*, 1998, **40**, 15
31 G. Zhang, T. Yamaguchi, H. Kawakami and T. Suzuki, *Appl. Catal. B*, 1992, **1**, L15